

# **CONTINUOUS PHOTOCATALYSIS SYSTEM IN THE DEGRADATION OF HERBICIDE**

A. Nathaporn, S. Vigneswaran\*, H. H. Ngo and J. Kandasamy

Faculty of Engineering, University of Technology, Sydney, P.O. Box 123, Broadway, NSW  
2007, Australia

\* Corresponding author Tel.: +612-9514 2641, Fax: +612-9514 2633, Email: s.vigneswaran@uts.edu.au

## **ABSTRACT**

The performance of both batch and continuous photo-catalytic reactors were studied to evaluate their capabilities in removing the sulfonyl urea herbicide of metsulfuron methyl (MM). It was found in a batch reactor, that an addition of a small amount of powder activated carbon (PAC) significantly increased the rate of degradation of MM. The continuous photo-catalytic system resulted in 57% of MM removal. When a small dose of activated carbon was added in the photo-catalytic system, MM removal increased to 78- 86% MM removal for detention times between of 5.25-21 min (corresponding to withdrawal rates of 10-40 mLmin<sup>-1</sup>). In this study, the pseudo first order rate constants of continuous photo-catalytic system revealed that shorter detention time were associated with lower rate constants. solid phase micro extraction/gas chromatography (SPME/GC) results showed that high concentrations of MM were broken down to small volatile organic compounds (VOCs) by photo-catalytic oxidation. PAC adsorbed the photo-products and increased the degradation of MM.

## **KEYWORDS**

metsulfuron methyl, heterogeneous photocatalysis, powder activated carbon, batch photo-catalytic reactor, continuous photo-catalytic reactor

## **1 INTRODUCTION**

Synthetic organic compounds (SOC) in water which include most of the herbicides are a major concern and causes health risks in water supply. Advanced treatment processes such as powder activated carbon (PAC) adsorption, granular activated carbon (GAC) adsorption, and nanofiltration are highly effective in removing the herbicides. Nanofiltration can remove between 50-90% herbicides and pesticides from water containing low concentration of natural organic matters  $0.4\text{--}3.6\text{ mgL}^{-1}$  (Agbekodo et al. [1]). PAC adsorption is effective in removing herbicides however it is expensive and does pose handling and disposal problems. Granular activated carbon (GAC) is an effective alternative to PAC and may be used in packed bed for the removal of herbicides.

Photo-catalytic oxidation is an alternative method for removing herbicide contaminant in water. Titanium dioxide ( $\text{TiO}_2$ ) is widely used as a photo-catalyst due to its low cost. It is non-toxic and photo-chemically stable. This process is based on the electronic excitation of a molecule or solid caused by light absorption e.g. UV light drastically alters its ability to lose or gain electrons and promote the decomposition of pollutants to harmless by-products (Molinari et al. [2]). Photo-induced electrons ( $e^-$ ) and positive holes ( $h^+$ ) are produced from  $\text{TiO}_2$  in the presence of UV light (Equation 1). These charged species can further generate free radicals (Equations 2 and 3). The highly oxidizing positive hole  $h^+$  resulting from the  $\text{TiO}_2$  photocatalysis is considered to be the dominant oxidizing species contributing to the mineralization process (Chu and Wong [3]).



In this study, the photo-catalytic oxidation process of metsulfuron methyl (MM) was investigated in the presence of TiO<sub>2</sub> and UV light. MM (C<sub>14</sub>H<sub>15</sub>N<sub>5</sub>O<sub>6</sub>S) is a widely used herbicide group B in Australia. The structure of MM is shown in Figure 1.

## **2 EXPERIMENTAL SET-UP**

The photocatalysis experiments were conducted using batch and continuous photo-reactors.

### **2.1 Batch Reactor**

The batch reactor used was equipped with three 8W UV lamps, air blower, and magnetic bar (Figure 2). The total surface area of the three lamps was 537 cm<sup>2</sup> and the volume of the reactor was 1.5 L. Air sparging was provided to supply oxygen into the reactor (3.3 VVM (air volume/solution volume/minute)). To ensure well mixed conditions in the reactor, magnetic stirring was used in addition to the air sparging. Tap water was circulated around the reactor to cool the reactor and control the temperature at 25 °C.

In the batch reactor, 3 UV lamps were arranged in a triangle to minimise the areas of overlap of irradiation between lamps (Masschelein and Rice [4]). The UV lamps used in the batch reactor experiments were the G8T5 germicidal lamps from Sankyo Denki. The intensity for low pressure mercury lamp reduces from the anode in the lower part of reactor to cathode at the upper part of the reactor. In general, the longer the lamp, the greater the exposure area is.

### **2.2 Continuous Photo-reactor**

The continuous mode photo-reactor used in this study is shown in Figure 3. The TiO<sub>2</sub> and UV lamps used here are the same as those used in the batch reactor experiments. In the continuous system the gap between lamp enclosure and the walls of cylindrical reactor was 3 mm

measured from the quart sleeve to the inside wall of the stainless steel reactor. The basic design conditions were adapted to ensure the following;

- In waste water treatment the flow must be turbulent ( $Re \geq 2000$ ) (Scheible et al. [5]). A circulation of  $150 \text{ mLmin}^{-1}$  (Q2 in Figure 3) was used to ensure turbulent conditions and to avoid the settling of  $\text{TiO}_2$  in the photocatalysis reactor.
- The pattern of flow through the UV reactors for disinfection should be plug flow (Thampi and Sorber [6])

Three stainless steel reactors with a volume of 70mL each were used giving a total volume of 210mL for the continuous reactor.  $\text{TiO}_2$  was dosed at a rate of  $1.5 \text{ gL}^{-1}$  directly into a holding tank (T1) containing 5 L of stock solution. The concentration of MM in the stock solution was  $10 \text{ mgL}^{-1}$  and it was mixed using a magnetic stirrer. One set of experiments were conducted with  $\text{TiO}_2$  alone while in another set of experiments a PAC dose of  $0.05 \text{ gL}^{-1}$  was added together with the  $\text{TiO}_2$ . Air sparging was also provided at the same rate as the batch reactor. The solution was then fed by a pump to a circulation tank (T2). Temperature in the recirculation tank was controlled by a thermoline in a holder tank. The solution containing  $\text{TiO}_2$  was pumped to the continuous photo-catalytic reactor at rates of 10, 20 and  $40 \text{ mLmin}^{-1}$ . It was recirculated in the photo-catalytic reactor at a rate of  $150 \text{ mLmin}^{-1}$  (Q2 in Figure 3) to prevent the settling of  $\text{TiO}_2$  and PAC within the reactor. The effluent withdrawal rate (Q1 in Figure 3) was adjusted to obtain the desired value of detention time where the detention time is equal to the volume of the photo-catalytic reactor divided by Q1. The effluent withdrawal rate in the continuous photo-reactor was set at 10, 20 and  $40 \text{ mLmin}^{-1}$  to allow detention times of 21, 10.5, 5.25 minutes respectively.

### 2.3 Chemicals

MM 60% herbicide group B purchased from Du Pont Australia was used to prepare the synthetic water. The initial concentration of MM in the synthetic water was  $10 \text{ mgL}^{-1}$ . All solutions were prepared using milli-q water (resistivity  $18 \text{ M}\Omega\text{-cm}$ ).

Titanium dioxide  $\text{TiO}_2$  – P25 A.R. grade was used as the photo-catalyst. It was purchased from Degussa Frankfurt, Germany. It is composed of 80% anatase and 20% rutile. The BET surface area is  $50 \pm 15 \text{ m}^2 \text{ g}^{-1}$ .

PAC (MD3545WB wood based powder) used in this study was purchased from James Cumming & Sons Pty Ltd., Australia. It had a mean pore diameter of 3.061 nm, a micropore volume of  $0.34 \text{ cm}^3 \text{ g}^{-1}$ , a mean diameter of 19.71  $\mu\text{m}$ , a maximum ash content of 6%, a maximum moisture content of 5%, and an iodine number of  $900 \text{ mgg}^{-1}$ .

### 2.4 Analysis

MM removal in the solution was measured in terms of total organic carbon (TOC) by using the Dohrmann Phoenix 8000 UV-persulfate TOC analyser with an autosampler. All samples were filtered through a  $0.45 \mu\text{m}$  membrane prior to the TOC measurement. Thus the TOC values obtained are, in fact, dissolved organic carbon (DOC) values.

The formation of nitrate, nitrite, and sulfate during the photo-catalytic reaction was monitored by suppressed ion chromatography Dionex DX – 600 which consists of: GP 50 gradient pump, ED50 A detector, AS 40 automated sampler with 0.5 mL sample vials, LC 30 Chromatography Oven with a rear – loading valve, AS 14 A anion separator column and an eluent alkaline buffer containing 8 mM sodium carbonate and 10 mM sodium bicarbonate.

A Varian Gas Chromatograph 3400 (GC) equipped with a flame ionization detector FID and a DB-5 (30 m length, 0.32 mm inner diameter) column J&W, Folsom, CA was utilized for all GC analyses. The stationary phase in the column consisted of cross-linked surface bonded 5% phenyl methylpolysiloxane with a film thickness of 1 $\mu$ m non-bonded. The system was operated using helium as the carrier gas with a linear velocity of 1 mLmin<sup>-1</sup>. The injector and detector temperatures were set at 280 °C. The only modification to the GC was the installation of a 0.75-mm diameter splitless glass inlet liner to increase the linear velocity of the flow and to leave less space for the analytes to reabsorb onto the SPME fibre. Both effects enhance desorption from the fibre.

Initial batch experiments focused on determining the time when equilibrium was established between the analytes in the stationary and aqueous phases. Triplicate solutions were extracted for periods of time ranging from 10 to 60 min of adsorption. The adsorption was assisted by using a magnetic stirrer in the 40 ml vial. The amount of adsorption was monitored after 10 min, 20 min, 30 min, 40 min, and 60 min. When the amount of adsorption did not increase any further, equilibrium was achieved. The peaks of SPME/GC chromatography after 30 minute, 40 minute, and 60 minutes of adsorption were similar indicating an equilibrium time of less than 30 minutes. Therefore, 30 min of adsorption was used throughout the study. The optimisation of the desorption temperature and time was investigated by considering the amount desorbed from fibres after extraction of analytes from a solution of known concentration and the subsequent carryover at a range of temperatures and time periods. The optimised conditions were to heat from 40 °C to 280 °C in the following manner. The initial column temperature was 40 °C. The temperature was increased to 100°C at a rate of increase of 10 °C per minute and hold time for 5 minutes, then to 250°C at a rate of increase of 30°C

per minute and hold time for 15 minutes, and finally to 280°C at a rate of increase of 10 °C per minute and hold time for 15 minutes. The total run time was 50 minutes.

### 3 RESULTS AND DISCUSSION

#### 3.1 Batch experiments

The results of batch experiments with TiO<sub>2</sub> and for PAC-TiO<sub>2</sub> are given in Table 1 and 2 respectively. The results are reported in terms of reduction in C/C<sub>0</sub> at different times upto 240 minutes. C<sub>0</sub> is the initial concentration of DOC and C is the corresponding concentration at a particular time.

Table 1 shows an initial lag stage of 30-60 min where the change in C/C<sub>0</sub> is small. This was principally due to the time required for adsorption of MM onto the surface of TiO<sub>2</sub>. This phenomenon was also observed by (Vulliet et al. [7]). After this lag stage, the photocatalytic reaction occurred progressively. The values of C/C<sub>0</sub> was found to decrease with TiO<sub>2</sub> dosage but remained relatively constant in the range of 0.5 to 2 gL<sup>-1</sup> for the experimental conditions used in this study.

Experiments with different doses of TiO<sub>2</sub> and the addition of a small amount of PAC 0.05 gL<sup>-1</sup> showed that the C/C<sub>0</sub> reduced significantly down to 0.24, Table 2. Further the reduction of C/C<sub>0</sub> occurred faster with the addition of PAC. The photocatalysis process was enhanced in the presence of PAC. The PAC adsorbed intermediate by-products produced during the photo-oxidation thereby enhancing the photocatalytic oxidation (Nathaporn et al. [8]). In the same manner displayed by the results of TiO<sub>2</sub> alone the values of C/C<sub>0</sub> was found to decrease initially with larger dosages of PAC-TiO<sub>2</sub> but remained relatively constant in the range of 0.5 to 1 gL<sup>-1</sup>.

### **3.2 Batch experiment - SPME/GC study characterisation of by products**

In this study, a detailed analysis with SPME/GC (solid phase micro extraction/gas chromatography) was made following batch photo-oxidation. Following 10 min of residence time in the batch reactor the MM partitioned to smaller molecular weight compounds (or substrate) which occurred at different peak times during the GC (12.09, 14.25, 17.35, 19.61 and 20.18 minutes), Figure 4. After 5 hours of residence time in batch reactor, some substrates degraded faster when activated carbon was used together with TiO<sub>2</sub>, Figure 5. The substrate that occurred at the peak times of 19.96 and 18.32 minutes during the GC had nearly disappeared, while the peak at time 14.27 minutes was lower. Maurino et al. [9] and Vulliet et al. [7] observed the final products of sulfonyl urea herbicides including MM were cynuric acid involving triazine moiety which hardly degrades and is harmless. Galletti et al. [10] observed MM using Varian 3400 gas chromatography (GC) equipped with Supelco SPB-5 coupled to a mass spectrophotometer. Their research showed the main products of MM were heterocyclic amine when the GC peak time occurred before 15 minutes (for the smaller molecular weight compound) and sulphonamide when the GC peak time occurred after 15 minute (for the larger molecular weight compound). In this study, both experiments were performed with the DB5 column of the GC using the same mobile phase conditions as Galletti et al. [10]. The peaks occurring in these experiments were similar to Galletti et al. [10] results. It was assumed substrates with a peak times of 14.2 and 12.09 are heterocyclic amine. For this study, MM was partially degraded after 5 hours of residence (operation) time to substrates with a GC peak times of 14.2 and 12.09 minutes. These by-products were assumed to be heterocyclic amine. If a biological metabolism process is utilised instead of photo-oxidation much more time would be required for degradation (Beyer et al. [11]).



The incomplete degradation of MM is more likely to lead to the mineralisation and formation of heterocyclic amine. Some of these by-products accumulated in solution and reduce the efficiency of photo-induced degradation, (Vulliet et al. [7]). Inclusion of PAC increases the adsorption of by-products that otherwise will accumulate in the solution and reduce the degradation rate.

### 3.3 The effect of inorganic compound in degradation of MM

During photo-oxidation, the sulphonamide ring of the herbicide breaks down into by products such as CO<sub>2</sub>, SO<sub>2</sub> and nitrogen species. In addition to this, NO<sub>3</sub><sup>-</sup> and SO<sub>4</sub><sup>2-</sup> of the herbicide were formed from hetero cyclic amide and sulfonamidic nitrogen of sulfonyl urea bridge respectively as shown in Equation (4) (Vulliet et al. [7]).



Nitrate and nitrite ions were formed as by photo-products as shown in Figure 6 (a). The formation of NO<sub>3</sub><sup>-</sup> and NO<sub>2</sub><sup>-</sup> anions occurred earlier when PAC was added in the photo-oxidation (Figure 6 (b)). The presence of nitrate and nitrite in the photo-reactor can contribute to the photo-oxidation as shown in Equations 5, 6 and 7 (Mark et al. [12]).



Similarly, SO<sub>4</sub><sup>2-</sup> ions form during the photo-oxidation of MM. Where PAC is present in the reactor the concentration of SO<sub>4</sub><sup>2-</sup> ions peaks earlier at approximately 50 min (Figure 7) and thereafter reduces in concentration. The reduction in concentration of SO<sub>4</sub><sup>2-</sup> after 50 min may be due to a portion being adsorbed on PAC-TiO<sub>2</sub> surface and a portion being transformed to SO<sub>2</sub> gas according to the photocatalytic reaction (Equation 4). With TiO<sub>2</sub> alone, the delayed reduction

in concentration of  $\text{SO}_4^{2-}$  occurring after 180 min reflects the smaller available absorbable area and active sites. Recent studies with synthetic organic compounds and herbicides of a similar nature showed that the presence of  $\text{SO}_4^{2-}$  ion inhibited the photo-catalytic oxidation (Hu et al. [13]; Wong and Chu [14]). The reduction in  $\text{SO}_4^{2-}$  ion means that photocatalysis is able to proceed at a faster rate. Arana et al. [15] attributed the increase in photocatalytic reaction of phenol, 4- amino phenol and salicylic acid to increased adsorption of photo-products on a larger BET surface available with activated carbon. In this study, the increase in efficiency of MM degradation is similarly attributed to the adsorption of photo-products on the larger BET surface available with  $\text{TiO}_2$  coupling with the PAC and active sites available to react with the pollutants. This reduces the competitive adsorption on active sites of PAC- $\text{TiO}_2$  increasing efficiency of degradation of MM. However, complicated photo-oxidation and by-products occur during these processes, and it was very difficult to determine the real mechanism of photo-catalytic reaction on the PAC- $\text{TiO}_2$  surface and the role of active sites because sophisticated instruments are required to confirm this.

### **3.4 Continuous photocatalysis system**

The effluent withdrawal rate in the continuous photo-reactor was set at 10, 20 and 40  $\text{mLmin}^{-1}$  to allow detention times of 21, 10.5 and 5.25 minutes respectively (Table 3). The total volume of photo-reactor was 210 mL. In the first set of experiments  $\text{TiO}_2$  was used alone while in the second set 0.05  $\text{gL}^{-1}$  of PAC was added together with the  $\text{TiO}_2$ .

In this study, the solution was mixed with the  $\text{TiO}_2$  and PAC catalyst for 15 min in the storage tank (T1 in Figure 3) in the absence of any light, before it was pumped to the circulation tank (T2). During this time, a small amount of DOC removal of 15% was noticed. This was due to the adsorption of MM onto the  $\text{TiO}_2$  and/or PAC as shown during the initial periods in Figure 8 a-c.

The DOC removal where TiO<sub>2</sub> was used alone was 56-57% (Table 3). DOC removal efficiency increased to between 78-86% when a small dose of PAC was added together with TiO<sub>2</sub> (Table 3). The removal efficiency at a detention time of 21 minutes (withdrawal rate of 10 mLmin<sup>-1</sup>) was approximately 69% after 65 minutes of operation time (Figure 8a). After that, there was a decrease in removal efficiency to 56% (Table 3). This decline in removal efficiency and overall low rate can be overcome by the addition of PAC as shown in Figure 8.

All the three experiments showed an increase in removal of DOC in the order of 20-30% when PAC was used together with TiO<sub>2</sub> similar to the batch reactor study. Furthermore the combined PAC- TiO<sub>2</sub> was able to achieve a high degradation of MM (DOC) of 78% even with at low detention times of 5.25 minutes. The removal occurs faster compared to where TiO<sub>2</sub> is used alone (Figure 8). This, continuous photocatalysis system yielded higher MM removal efficiency with greater flexibility.

### 3.5 DOC removal rates

The DOC removal for the continuous system was measured with time for different doses of TiO<sub>2</sub> alone and for doses of PAC-TiO<sub>2</sub>. The concentration of DOC was plotted in the form of ln(C/C<sub>0</sub>) against the time where C<sub>0</sub> is the initial concentration of DOC and C is the concentration at a particular time. The plot shows a near linear trend after an initial period of preliminary adsorption, (Figure 9).

The rate expression of Langmuir – Hinshewood (L-H) (Equation (8)) (Bhattacharyya et al. [16]; Bianco Prevot et al. [17]; Kartal et al. [18]; Vulliet et al. [7]) is given by

$$R = -\frac{dC}{dt} = \frac{K_{Ad}kC_0}{1 + K_{Ad}C_0} \quad (8)$$

where  $C_0$  = initial concentration

$K_{Ad}$  = the adsorption coefficient

$k$  = reaction rate constant

Integrating Equation 8 for low initial concentration of MM gives the following equation

$$\ln(C_t/C_0) = -K_{Ad}kt = k^*t \quad (9)$$

where:  $k^*$  = pseudo first order rate constant,  $\text{min}^{-1}$ ,  $C_0$  and  $C_t$  are the initial and final concentration of the MM.

From the temporal variation of DOC removal, the pseudo first order degradation rate was calculated for each dose of  $\text{TiO}_2$  and similarly for each dose of PAC- $\text{TiO}_2$ . The pseudo first-order constants determined and the corresponding linear regression coefficient are tabulated in Table 4. The reaction rate increased significantly with the addition of PAC (Figure 9b). Comparison between  $\ln(C/C_0)$  of DOC versus time for  $\text{TiO}_2$  alone (60 minutes operation time) and for PAC- $\text{TiO}_2$  (35 minutes operation time) shows a higher pseudo first order rate constant in the later. A shorter duration was used in the later because of the faster rate at which it degrades.

Tables 4 and 5 show the variation of rate constant ( $k^*$ ) for the range of withdrawal rates tested. A reduction in detention time corresponds to a decrease in the pseudo first order rate constant for  $\text{TiO}_2$  from  $0.0168 \text{ min}^{-1}$  for a detention time of 21 minutes to  $0.0089 \text{ min}^{-1}$  for detention time of 5.25 minutes (Table 3). The pseudo first order rate constants of PAC- $\text{TiO}_2$  increased when detention time increased from  $0.0142$  (5.2 minutes detention time) to  $0.0357$  (21 minutes detention time). However, there also a commensurate increase in the DOC removal 78% (5.2 minute detention time) to 86% (21 minute detention time).

## **4 CONCLUSION**

### **4.1 Batch reactor**

The photo-products of MM revealed higher rates of degradation of MM by using PAC- TiO<sub>2</sub>. Higher inorganic products of MM such as NO<sub>2</sub><sup>-</sup>, NO<sub>3</sub><sup>-</sup> and SO<sub>4</sub><sup>2-</sup> and small organic photo-products were produced during photo-oxidation of MM. Inorganic compounds such as SO<sub>4</sub><sup>2-</sup> can inhibit photocatalysis. The increase in efficiency of MM degradation is attributed to the adsorption of photo-products on the larger BET surface available with PAC-TiO<sub>2</sub> and active sites available to react with the pollutants. This reduces the competitive adsorption on active sites of PAC-TiO<sub>2</sub> increasing efficiency of degradation of MM.

### **4.2 Continuous reactor**

The coupling of PAC with continuous heterogeneous photocatalysis leads to faster degradation of MM than the heterogeneous photocatalysis alone. The incorporation of a small amount of PAC of 0.05 gL<sup>-1</sup> with TiO<sub>2</sub> of 1.5 gL<sup>-1</sup> led to 78% removal even with a short residence time of 5.25 minutes. The major problems of degrading herbicide and persistent organic compounds are the long period of contact time and difficult degradation. With PAC-TiO<sub>2</sub> continuous photocatalysis system, faster detention time and the higher removal efficiency were achieved. The system operated at a range of flows with high removal efficiency gives more flexibility for coupling with hybrid systems such as a membrane process.

## **5 ACKNOWLEDGMENT**

The research is funded by Australia Research Council Discovery Grant. The first author thanks the Royal Thai Government for providing scholarship to pursue this work.

## 6 REFERENCE

- [1] K.M. Agbekodo, B. Legube, and S. Dard, Atrazine and simazine removal mechanisms by nanofiltration: Influence of natural organic matter concentration, *Water Research*, 30(11), 2535-2542.
- [2] R. Molinari, M. Borgese, E. Drioli, L. Palmisano and M. Schiavello, Hybrid processes coupling photocatalysis and membranes for degradation of organic pollutants in water, *Catalysis Today*, 75(1-4), 77-85.
- [3] W. Chu, and C.C. Wong, The photocatalytic degradation of dicamba in TiO<sub>2</sub> suspensions with the help of hydrogen peroxide by different near UV irradiations, *Water Research*, 38(4), 1037-1043.
- [4] W.J. Masschelein and R.G. Rice, *Ultraviolet Light in Water and Wastewater Sanitation*, Lewis Publishers, Boca Raton, Florida.
- [5] O.K. Scheible, M.C. Casey and A. Fondran, *National Technical Information Service*, NITS Publication 86 - 145182
- [6] M.V.Thampi and C.A. Sorber, A method for evaluating the mixing characteristics of u.v. reactors with short detention times, *Water Research*, 21(7), 765-771.
- [7] E. Vulliet, C. Emmelin, J.-M Chovelon, C.Guillard, and J.-M.Herrmann, Photocatalytic degradation of the herbicide cinosulfuron in aqueous TiO<sub>2</sub> suspension, *Environ Chem Lett*, 1, 62 - 67.
- [8] A. Nathaporn, H. K. Shon, S. Vigneswaran and H.H Ngo, Photocatalytic hybrid system in degradation of herbicide (metsulfuron-methy), *Water Science and Technology: Water supply*, 6(2), 109 -114.
- [9] V. Maurino, C. Minero, E. Pelizzetti and M. Vincenti, M, Photocatalytic transformation of sulfonylurea herbicides over irradiated titanium dioxide particles, *Colloids and Surfaces A: Physicochemical and Engineering Aspects*, 151(1-2), 329-338.

- [10] G.C. Galletti, G. Chiavari, F.A. Mellon, and K. Parlsey, Pyrolysis gas chromatography /mass spectrometry and electron impact-fast atom bombardment-mass spectrometry of sulfonylureas, *Journal of Analytical and Applied Pyrolysis*, 21(1-2), 239-247.
- [11] E.M. Beyer, M.J. Duffy, J.V. Hay and D.D Schlueter, Sulfonylurea herbicides, in: Herbicides: ." *Chemistry, Degradation , and Mode of Action*, 3, pp. 117-189.
- [12] G. Mark, H.-G. Korth, H.-P Schuchmann and C. von Sonntag, The photochemistry of aqueous nitrate ion revisited, *Journal of Photochemistry and Photobiology A: Chemistry*, 101(2-3), 89-103.
- [13] C. Hu, T. Yuchao, L. Lanyu, H. Zhengping and T. Hongxiao, Effects of inorganic anions on photoactivity of various photocatalysts under different conditions, *Journal of Chemical Technology and Biotechnology*, 79, P. 247-252.
- [14] C.C Wong and W. Chu, W. (2003), The direct photolysis and photocatalytic degradation of alachlor at different TiO<sub>2</sub> and UV sources, *Chemosphere*, 50(8), 981-987.
- [15] J. Arana, J.M. Dona-Rodriguez, E. Tello Rendon, C. Garriga i Cabo, O. Gonzalez-Diaz, J.A. Herrera-Melian, J. Perez-Pena, G. Colon, and J.A. Navio, TiO<sub>2</sub> activation by using activated carbon as a support: Part I. Surface characterisation and decantability study, *Applied Catalysis B: Environmental*, 44(2), 161-172.
- [16] A. Bhattacharyya, S. Kawi, and M.B. Ray, Photocatalytic degradation of orange II by TiO<sub>2</sub> catalysts supported on adsorbents, *Catalysis Today*, In Press, Corrected Proof.
- [17] A. Bianco Prevot, M. Vincenti, A. Bianciotto, and E. Pramauro, Photocatalytic and photolytic transformation of chloramben in aqueous solutions, *Applied Catalysis B: Environmental*, 22(2), 149-158.
- [18] Ö. E Kartal, M. Erol and H. Oğluz, Photocatalytic Destruction of Phenol by TiO<sub>2</sub> Powders, *Chemical Engineering & Technology*, 24(6), p 645-649.

## LIST OF TABLES

Table 1 Values of  $C/C_0$  of DOC for different concentration of  $TiO_2$

Table 2 Values of  $C/C_0$  of DOC for  $TiO_2/PAC$ .

Table 3. DOC removal at different detention time (MM concentration =  $10\text{ mgL}^{-1}$ ,  $TiO_2$  =  $1.5\text{ GL}^{-1}$ , PAC =  $0.05\text{ gL}^{-1}$ )

Table 4 Variation of pseudo first order rate constant obtained from Equation (9) at different withdrawal rates of  $1.5\text{ gL}^{-1}\text{ TiO}_2$

Table 5 Variation of pseudo first order rate constant obtained from Equation (9) at different withdrawal rate of  $1.5\text{ gL}^{-1}\text{ TiO}_2$  and  $0.05\text{ gL}^{-1}\text{ PAC}$



## LIST OF FIGURES

Figure 1. The structure of Metsulfuron-methyl (MM)

Figure 2. Schematic of the photo-catalytic batch reactor

Figure 3. Schematic of the continuous flow photo-catalytic reactor with the catalyst

(T1: Mixing tank with no light source; Q1: influent and withdrawal rate; Q2: re-circulation flow; T2: re-circulation tank; R: photo-catalytic reactor unit; L1, L2, L3 are UV lamps of 8 watts each)

Figure 4. 10min SPME/GC chromatogram of MM with  $\text{TiO}_2$   $1.5\text{gL}^{-1}$

Figure 5. 5 hours SPME/GC chromatogram of MM with  $\text{TiO}_2$   $1.5\text{gL}^{-1}$

Figure 6. Formation of (a) nitrate and (b) nitrite during the batch photocatalysis batch system ( $1\text{gL}^{-1}$  of  $\text{TiO}_2$  alone (solid line) and  $1\text{gL}^{-1}$   $\text{TiO}_2$  with  $0.05\text{gL}^{-1}$  of PAC (dotted line))

Figure 7. Formation of sulfate anion by using  $\text{TiO}_2$   $1\text{gL}^{-1}$  (solid line) and  $1\text{gL}^{-1}$   $\text{TiO}_2$  with PAC  $0.05\text{gL}^{-1}$  (dotted line)

Figure 8 a-c. DOC removal by continuous photo-catalytic reactor

Figure 9 a-b. Test of pseudo- first order rate constants according to Equation (9) at different withdrawal rate and (a) with  $\text{TiO}_2$  alone and (b)  $\text{TiO}_2$  and  $0.05\text{gL}^{-1}$  PAC.

Table 1 Values of  $C/C_0$  of DOC for different concentration of  $TiO_2$

| Time<br>(min) | Values of $C/C_0$ of DOC for different concentration of $TiO_2$ |                  |                  |                |
|---------------|-----------------------------------------------------------------|------------------|------------------|----------------|
|               | 0.1<br>$gL^{-1}$                                                | 0.5<br>$gL^{-1}$ | 1.0<br>$gL^{-1}$ | 2<br>$gL^{-1}$ |
| 10            | 0.92                                                            | 0.96             | 0.83             | 0.92           |
| 20            | 0.93                                                            | 0.97             | 0.86             | 0.86           |
| 30            | 0.94                                                            | 0.93             | 0.86             | 0.88           |
| 60            | 0.95                                                            | 0.70             | 0.82             | 0.74           |
| 120           | 0.84                                                            | 0.55             | 0.68             | 0.57           |
| 180           | 0.75                                                            | 0.43             | 0.53             | 0.47           |
| 240           | 0.64                                                            | 0.39             | 0.31             | 0.33           |

Table 2 Values of  $C/C_0$  of DOC for  $TiO_2/PAC$ .

| Time<br>(min) | Values of $C/C_0$ of DOC for concentrations of $TiO_2/PAC$ |                   |                   |                 |
|---------------|------------------------------------------------------------|-------------------|-------------------|-----------------|
|               | 0.1*<br>$gL^{-1}$                                          | 0.3*<br>$gL^{-1}$ | 0.5*<br>$gL^{-1}$ | 1*<br>$gL^{-1}$ |
| 10            | 0.73                                                       | 0.67              | 0.69              | 0.67            |
| 30            | 0.67                                                       | 0.58              | 0.69              | 0.67            |
| 60            | 0.62                                                       | 0.52              | 0.58              | 0.53            |
| 120           | 0.54                                                       | 0.43              | 0.50              | 0.47            |
| 180           | 0.46                                                       | 0.38              | 0.36              | 0.42            |
| 240           | 0.41                                                       | 0.37              | 0.24              | 0.28            |

\* The concentration of  $TiO_2$  is as indicated and the concentration of PAC is  $0.05\ gL^{-1}$

Table 3. DOC removal at different detention time (MM concentration =10 mgL<sup>-1</sup>, TiO<sub>2</sub> = 1.5 gL<sup>-1</sup>, PAC = 0.05 gL<sup>-1</sup>)

| Withdrawal rate<br>(mLmin <sup>-1</sup> ) | Detention time<br>(min) | % DOC removal<br>(TiO <sub>2</sub> /UV) | % DOC removal<br>(TiO <sub>2</sub> /UV/PAC) |
|-------------------------------------------|-------------------------|-----------------------------------------|---------------------------------------------|
| 10                                        | 21                      | 57                                      | 86                                          |
| 20                                        | 10.5                    | 57                                      | 81                                          |
| 40                                        | 5.25                    | 56                                      | 78                                          |

Table 4 Variation of pseudo first order rate constant obtained from Equation (9) at different withdrawal rates of  $1.5 \text{ gL}^{-1} \text{ TiO}_2$

| Withdrawal rate<br>( $\text{mLmin}^{-1}$ ) | Detention time<br>(min) | $k^*$<br>( $\text{min}^{-1}$ ) | $R^2$ |
|--------------------------------------------|-------------------------|--------------------------------|-------|
| 10                                         | 21                      | 0.0168                         | 0.87  |
| 20                                         | 10.5                    | 0.0098                         | 0.86  |
| 40                                         | 5.25                    | 0.0089                         | 0.72  |

Table 5 Variation of pseudo first order rate constant obtained from Equation (9) at different withdrawal rate of 1.5 gL<sup>-1</sup> TiO<sub>2</sub> and 0.05 gL<sup>-1</sup> PAC

| Withdrawal rate<br>(mLmin <sup>-1</sup> ) | Detention time<br>(min) | k<br>(min <sup>-1</sup> ) | R <sup>2</sup> |
|-------------------------------------------|-------------------------|---------------------------|----------------|
| 10                                        | 21                      | 0.0357                    | 0.99           |
| 20                                        | 10.5                    | 0.0251                    | 0.87           |
| 40                                        | 5.25                    | 0.0142                    | 0.99           |

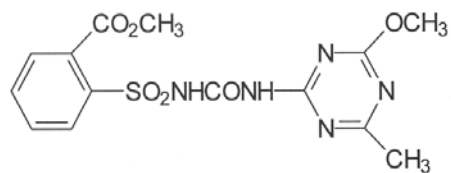


Figure 1. The structure of Metsulfuron-methyl (MM)

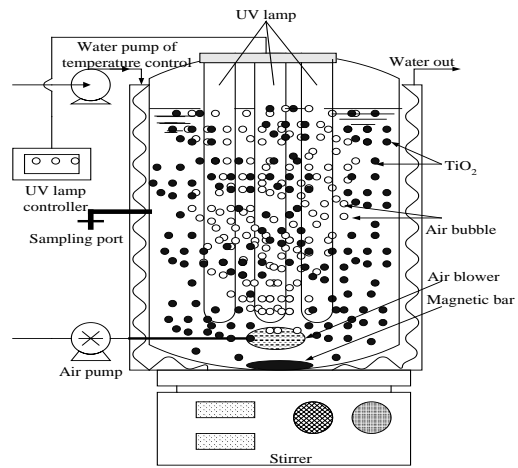


Figure 2. Schematic of the photo-catalytic batch reactor



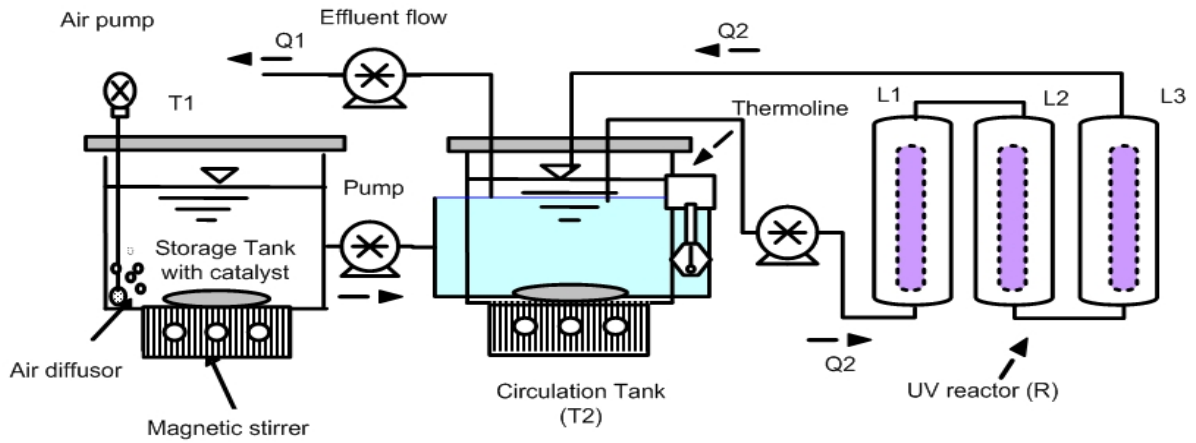


Figure 3 Schematic of the continuous flow photo-catalytic reactor with the catalyst (T1: Mixing tank with no light source; Q1: influent and withdrawal rate; Q2: re-circulation flow; T2: re-circulation tank; R: photo-catalytic reactor unit; L1, L2, L3 are UV lamps of 8 watts each)

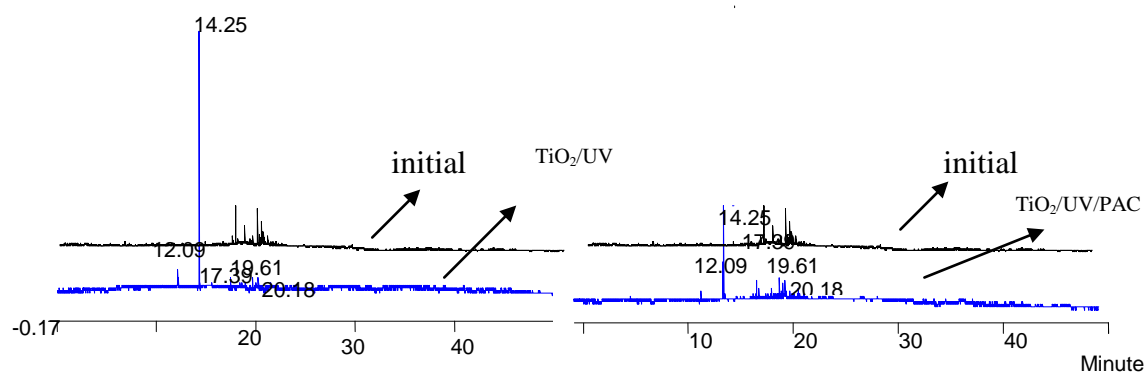


Figure 4. Ten minute SPME/GC chromatogram of MM with  $\text{TiO}_2$   $1.5 \text{ gL}^{-1}$

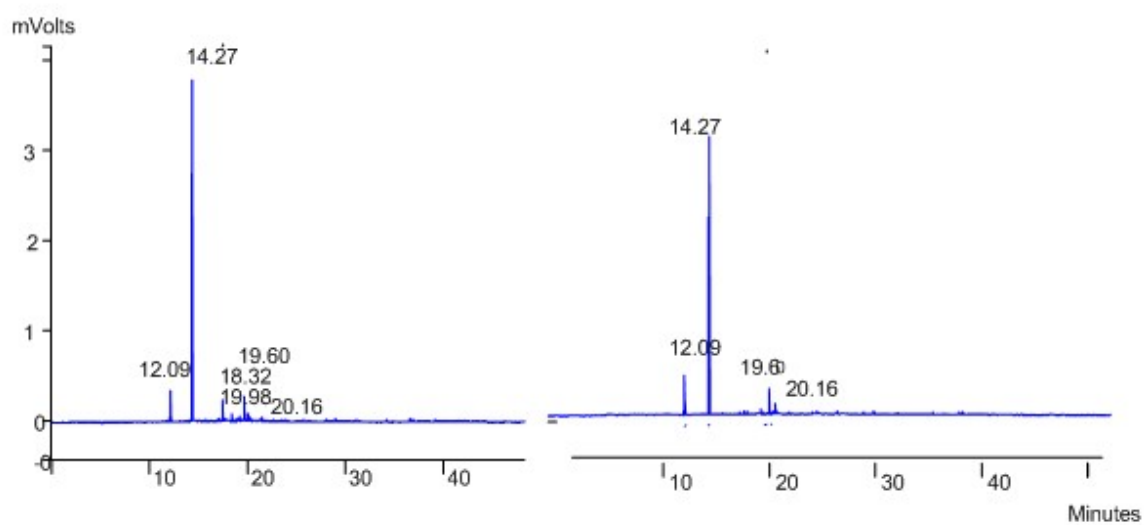
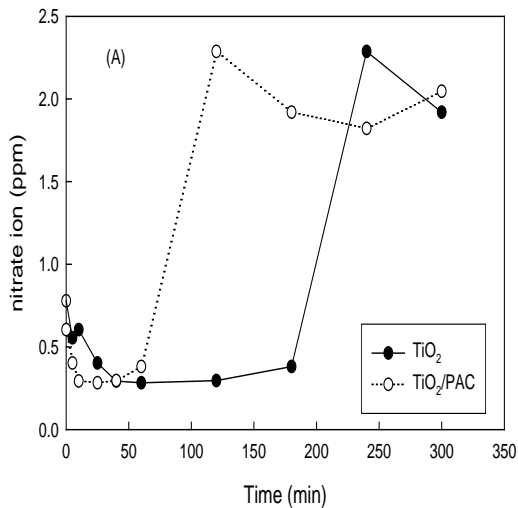
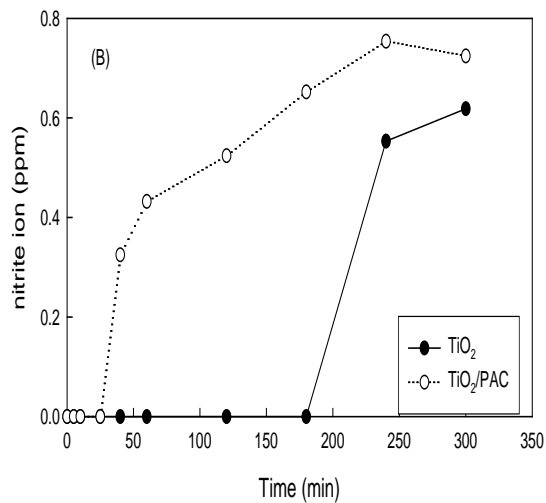


Figure 5. Five hour SPME/GC chromatogram of MM with  $\text{TiO}_2$   $1.5 \text{ gL}^{-1}$



(a) nitrate



(b) nitrite

Figure 6. Formation of (a) nitrate and (b) nitrite during the batch photocatalysis batch system ( $1 \text{ gL}^{-1}$  of  $\text{TiO}_2$  alone (solid line) and  $1 \text{ gL}^{-1}$   $\text{TiO}_2$  with  $0.05 \text{ gL}^{-1}$  of PAC (dotted line))

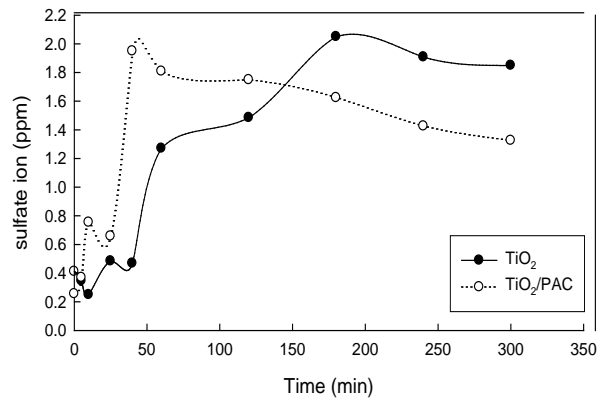
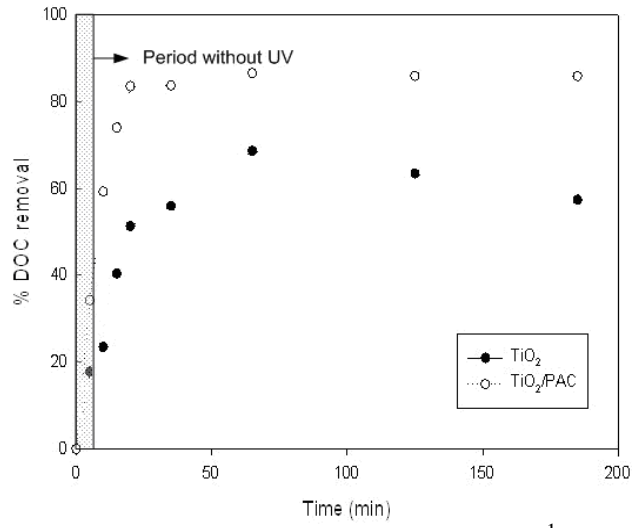
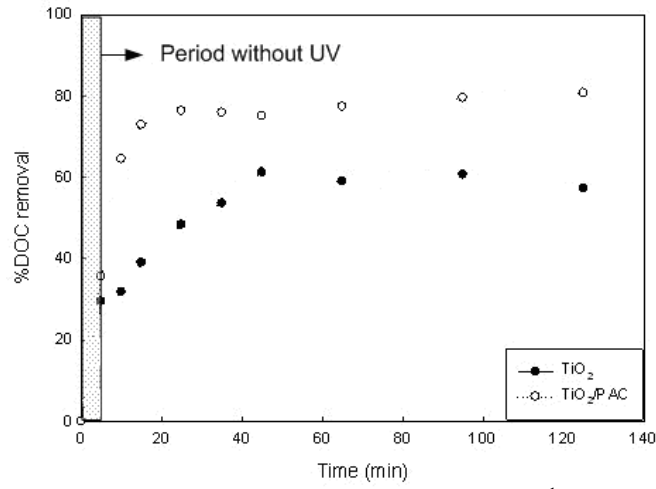


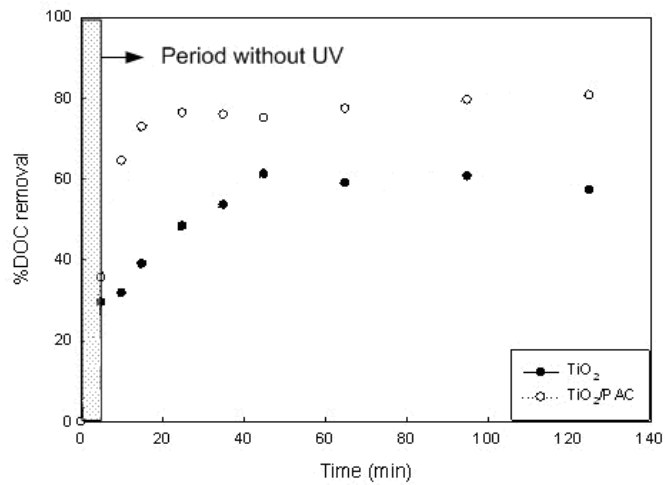
Figure 7. Formation of sulfate anion by using  $\text{TiO}_2 1 \text{ gL}^{-1}$  (solid line) and  $1 \text{ gL}^{-1} \text{ TiO}_2$  with PAC  $0.05 \text{ gL}^{-1}$  (dotted line)



(a) withdrawal rate of 10 mLmin<sup>-1</sup>

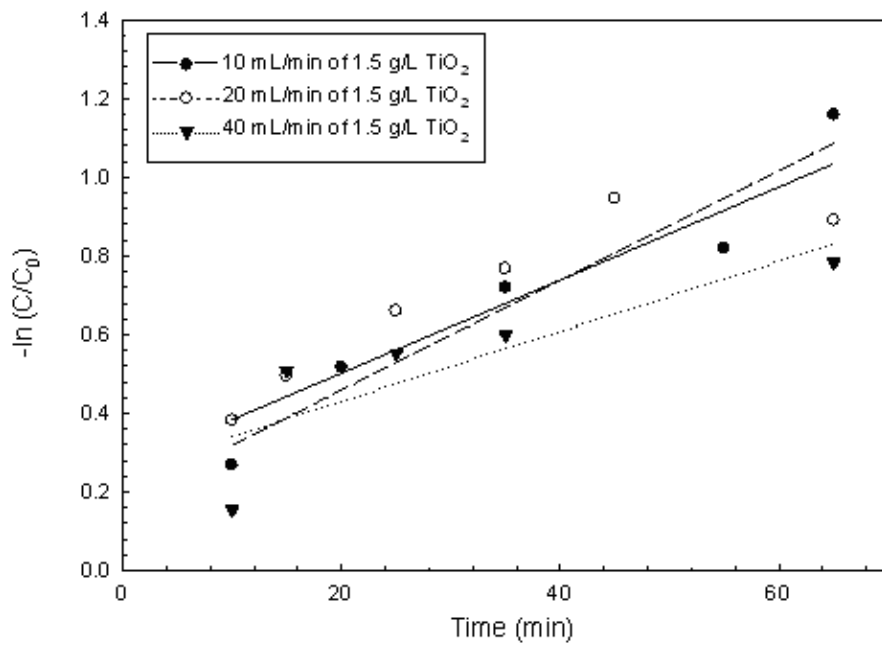


(b) withdrawal rate of 20 mLmin<sup>-1</sup>

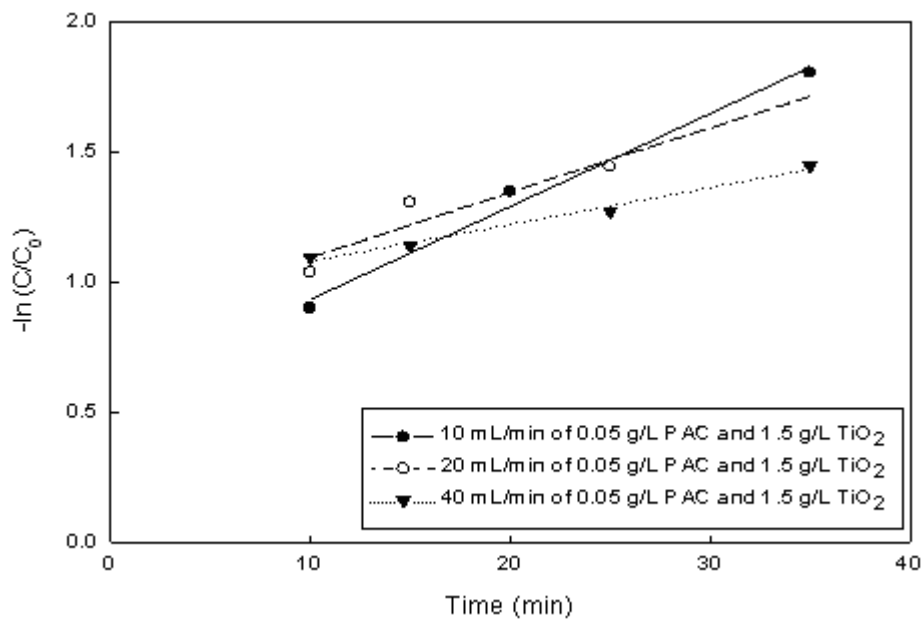


(c) withdrawal rate of 40 mLmin<sup>-1</sup>

Figure 8(a-c) DOC removal by continuous photo-catalytic reactor



(a) 1.5 gL<sup>-1</sup> of TiO<sub>2</sub>



(b) 0.05 gL<sup>-1</sup> PAC and 1.5 gL<sup>-1</sup> of TiO<sub>2</sub>

Figure 9 a-b. Test of pseudo- first order rate constants according to Equation (9) at different withdrawal rate and (a) with TiO<sub>2</sub> alone and (b) TiO<sub>2</sub> and 0.05 gL<sup>-1</sup> PAC.